Effect of biaxial strain on acceptor-level energies in $In_yGa_{1-y}As/Al_xGa_{1-x}As$ (on GaAs) quantum wells

J. P. Loehr and J. Singh
Center for High Frequency Microelectronics, Department of Electrical Engineering and Computer Science, College of Engineering, The University of Michigan, Ann Arbor, Michigan 48109-2122
(Received 6 October 1989)

Biaxial compressive strain produced in pseudomorphic epitaxy is known to alter the valence-band structure considerably. A theoretical formalism is presented to study the consequences of strain on carrier masses and hydrogenic acceptor levels in quantum wells. Using a nonvariational numerical method, we calculate the acceptor binding energy in an $Al_xGa_{1-x}As/In_yGa_{1-y}As$ quantum well as a function of indium content and position of the acceptor impurity in the well. The acceptor-level energy is found to be a strong function of strain and could be used as a signature to study the valence-band structure.

I. INTRODUCTION

The effect of strain on the electronic band structure of semiconductors has been an area of intense research for several years. Recently, this area has attracted considerable renewed interest due to the ability to epitaxially grow lattice-mismatched layers. Theoretical and experimental studies show that if a material with bulk lattice constant α_L is grown as a thin film on a thick substrate of different lattice constant α_s, the film will grow pseudomorphically up to a critical thickness above which lattice coherence will be lost with dislocation generation.[1] In the pseudomorphic regime, the in-plane lattice constant of the overlayer is the same as that of the substrate while the perpendicular lattice constant adjusts via the Poisson effect producing a built-in strain. A consequence of this strain is the change in the band structure and carrier masses accompanied by degeneracy lifting at certain points.[2–5] In particular, the valence band is dramatically affected, especially near the band edges. These changes are reflected in lowering of the hole masses in biaxial compressively strained quantum wells. The improved hole properties in strained quantum wells are useful for electronic and optical devices. At present there have been no studies of acceptor levels in the strained quantum well, although work on lattice-matched quantum wells has been reported.[6]

In this paper we will examine the effect of biaxial strain on hydrogenic acceptor levels in $Al_xGa_{1-x}As/In_yGa_{1-y}As$ quantum wells. In Sec. II we present a nonvariational numerical technique which allows us to solve the acceptor problem in arbitrary quantum-well profiles as a function of strain and dopant position in the well. We present the results of our calculations in Sec. III. In particular, we show that acceptor-level energies can be an important guide to the valence-band structure in strained quantum wells and we conclude in Sec. IV.

II. THEORETICAL FORMALISM

In this section we discuss the effect of strain on the valence-band structure of a pseudomorphically strained quantum well. The acceptor-level problem is also discussed and its solution via a nonvariational numerical technique is presented.

A. Effect of strain on quantum-well band structure

In bulk III-V compound semiconductors the top of the valence band is fourfold degenerate and at the Brillouin-zone center the eigenstates have pure angular momentum character corresponding to $|\frac{3}{2},\pm\frac{3}{2}\rangle$ heavy-hole (hh) and $|\frac{3}{2},\pm\frac{1}{2}\rangle$ light-hole (lh) states. In GaAs the split-off band ($|\frac{1}{2},\pm\frac{1}{2}\rangle$) is far enough removed that its effect on most hole-related properties can be ignored. To describe the valence-band structure in quantum wells, it is important to retain the mixing of hh and lh states since the states mix very strongly away from $\mathbf{k}=\mathbf{0}$. We choose to describe the valence-band states via the degenerate $\mathbf{k}\cdot\mathbf{p}$ formalism which accurately accounts for the mixing.[7] In this the hole state $|m,\mathbf{k}\rangle$ is given by

$$\langle \mathbf{r}_h|m,\mathbf{k}\rangle=\frac{e^{i\mathbf{k}\cdot\boldsymbol{\rho}_h}}{2\pi}\sum_{\nu} g_m^{\nu}(\mathbf{k},z_h)U_0^{\nu}(\mathbf{r}_h)\ , \tag{1}$$

where $\mathbf{k}$ is the in-plane two-dimensional wave vector, $\boldsymbol{\rho}_h$ is the in-plane radial coordinate, z_h is the coordinate in the growth direction, the U_0^{ν} are the zone-center Bloch functions having spin symmetry ν, and m is a subband index. The envelope functions $g_m^{\nu}(\mathbf{k},z_h)$ and subband energies $E_m(\mathbf{k})$ satisfy

$$\begin{bmatrix} H_{hh}+\frac{1}{2}\delta & b & c & 0 \\ b^{\dagger} & H_{lh}-\frac{1}{2}\delta & 0 & c \\ c^{\dagger} & 0 & H_{lh}-\frac{1}{2}\delta & -b \\ 0 & c^{\dagger} & -b^{\dagger} & H_{hh}+\frac{1}{2}\delta \end{bmatrix} \begin{bmatrix} g_m^{3/2,3/2}(\mathbf{k},z_h) \\ g_m^{3/2,1/2}(\mathbf{k},z_h) \\ g_m^{3/2,-1/2}(\mathbf{k},z_h) \\ g_m^{3/2,-3/2}(\mathbf{k},z_h) \end{bmatrix} = E_m(\mathbf{k}) \begin{bmatrix} g_m^{3/2,3/2}(\mathbf{k},z_h) \\ g_m^{3/2,1/2}(\mathbf{k},z_h) \\ g_m^{3/2,-1/2}(\mathbf{k},z_h) \\ g_m^{3/2,-3/2}(\mathbf{k},z_h) \end{bmatrix} . \quad (2)$$

Here δ is the separation of the hh and lh states in a bulk material due to the strain. For the $In_yGa_{1-y}As$ system it is given by $\delta=-5.966\varepsilon$, where ε is the lattice mismatch between the well and the $Al_xGa_{1-x}As$ barrier.[3] Note that the functions $g_m^{\nu}(\mathbf{k},z_h)$ depend on $\mathbf{k}$ as well as z_h and that the energy bands are not, in general, parabolic. The matrix entries in Eq. (2) are given by[4]

$$H_{hh}=-\frac{\hbar^2}{2m_0}\left[(k_x^2+k_y^2)(\gamma_1+\gamma_2)-(\gamma_1-2\gamma_2)\frac{\partial^2}{\partial z_h^2}\right] + V^h(z_h) , \quad (3)$$

$$H_{lh}=-\frac{\hbar^2}{2m_0}\left[(k_x^2+k_y^2)(\gamma_1-\gamma_2)-(\gamma_1+2\gamma_2)\frac{\partial^2}{\partial z_h^2}\right] + V^h(z_h) , \quad (4)$$

$$c=-\frac{\sqrt{3}\hbar^2}{2m_0}[\gamma_2(k_x^2-k_y^2)-2i\gamma_3 k_x k_y] , \quad (5)$$

$$b=\frac{i\sqrt{3}\hbar^2}{m_0}(-k_y-ik_x)\gamma_3\frac{\partial}{\partial z_h} , \quad (6)$$

where m_0 is the free-electron mass, V^h is the potential profile for the hole, and for GaAs $\gamma_1=6.85$, $\gamma_2=2.1$, and $\gamma_3=2.9$.

We solve Eq. (2) by writing it in finite difference form and diagonalizing the resulting matrix to obtain the in-plane band structure.[4] Figure 1 shows the [100] band structure for a 100 Å quantum well confined by $Al_{0.3}Ga_{0.7}As$. The well region is lattice matched GaAs for Fig. 1(a) and $In_{0.2}Ga_{0.8}As$ for Fig. 1(b); all the bands are doubly degenerate. The effect of the strain is evident in the sharper curvature at the zone center in Fig. 1(b). Away from the zone center, though, the curvatures are similar for the strained and unstrained cases. As a result, the change in the acceptor-level energy is not as great as the change in the near-band-edge hole mass, since the acceptor is made up of states from all $\mathbf{k}$, while the effective mass reflects only the curvature of the bands near the zone center.

In Figs. 2 and 3 we plot the probability density function $\sum_{\nu}|g_m^{\nu}(\mathbf{k},z_h)|^2$ as a function of k and z_h with $\mathbf{k}$ along the [100] direction for a 100-Å GaAs quantum well confined by $Al_{0.3}Ga_{0.7}As$. Figures 2(a) and 2(b) correspond to the two different eigenfunctions of the doubly degenerate energies. Figure 2 shows the form of the probability density for the two spin-degenerate states of the first heavy-hole band (hh1). We see that there is a significant change in the functions as k changes and that there is also a slight asymmetry between the two spin-pair states. In Fig. 3 we show the two degenerate states of the first light-hole band (lh1). Again, the probability density changes dramatically with k and there is also a substantial asymmetry between the two degenerate states. The sharp change in the functions at $k\approx 0.10/\text{Å}$ reflects the crossing of the hh1 and lh1 bands in Fig. 1(a). For higher-order subbands, the qualitative change in the wave functions with k and the asymmetry between degenerate states is even more extreme. We will show below that

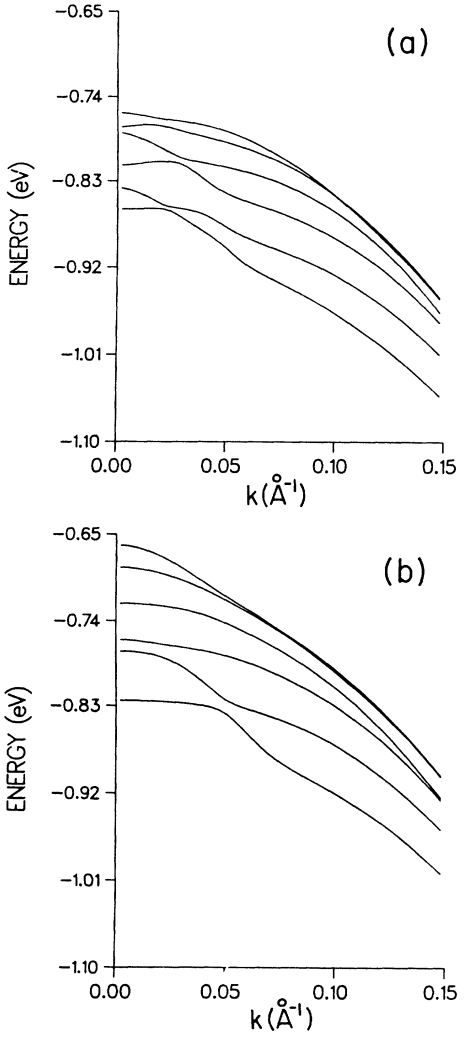

FIG. 1. Valence-band structure in a 100-Å (a) GaAs/$Al_{0.3}Ga_{0.7}As$ and (b) $In_{0.2}Ga_{0.8}As/Al_{0.3}Ga_{0.7}As$ quantum well.

this asymmetry in z_h results in a splitting of the acceptor levels for off-center impurities.

B. The acceptor problem

When solving the acceptor problem for an impurity located at z_i, we want to consider the nonparabolicity of the valence band *and* the variation with $\mathbf{k}$ of the envelope functions $g_m^\nu(\mathbf{k},z_h)$. These effects are most easily incorporated by solving the problem in $\mathbf{k}$ space; i.e., we directly diagonalize the impurity potential

$$V(\boldsymbol{\rho};z_i,z_h)=\frac{-e^2}{\epsilon[\rho^2+(z_i-z_h)^2]^{1/2}}$$

in the $|m,\mathbf{k}\rangle$ basis. To do this, we must know the form of the matrix elements $\langle m,\mathbf{k}|V|m',\mathbf{k}'\rangle$. From arguments similar to those used in Ref. 7 to derive Eq. (2), it can be shown that the zone-center Bloch functions $U_0^\nu(\mathbf{r}_h)$ serve to connect only functions g_m^ν with the same spin index ν, so we have

$$\langle m,\mathbf{k}|V|m',\mathbf{k}'\rangle = \int dz_h \sum_\nu g_m^{\nu *}(\mathbf{k},z_h)g_{m'}^\nu(\mathbf{k}',z_h)V(\mathbf{k}-\mathbf{k}';z_i,z_h)\ , \quad (7)$$

where

$$V(\mathbf{k}-\mathbf{k}';z_i,z_h)\equiv\frac{1}{(2\pi)^2}\int d\boldsymbol{\rho}'\, e^{-i(\mathbf{k}-\mathbf{k}')\cdot\boldsymbol{\rho}'}V(\boldsymbol{\rho}';z_i,z_h)$$
$$=\frac{-e^2}{2\pi\epsilon|\mathbf{k}-\mathbf{k}'|}e^{|\mathbf{k}-\mathbf{k}'||z_i-z_h|}\ . \quad (8)$$

To solve the acceptor problem, we start with the zeroth-order hole solutions from Eq. (1):

$$H^0|m,\mathbf{k}\rangle=E_m(\mathbf{k})|m,\mathbf{k}\rangle\ . \quad (9)$$

When we take the impurity-hole interaction into account,

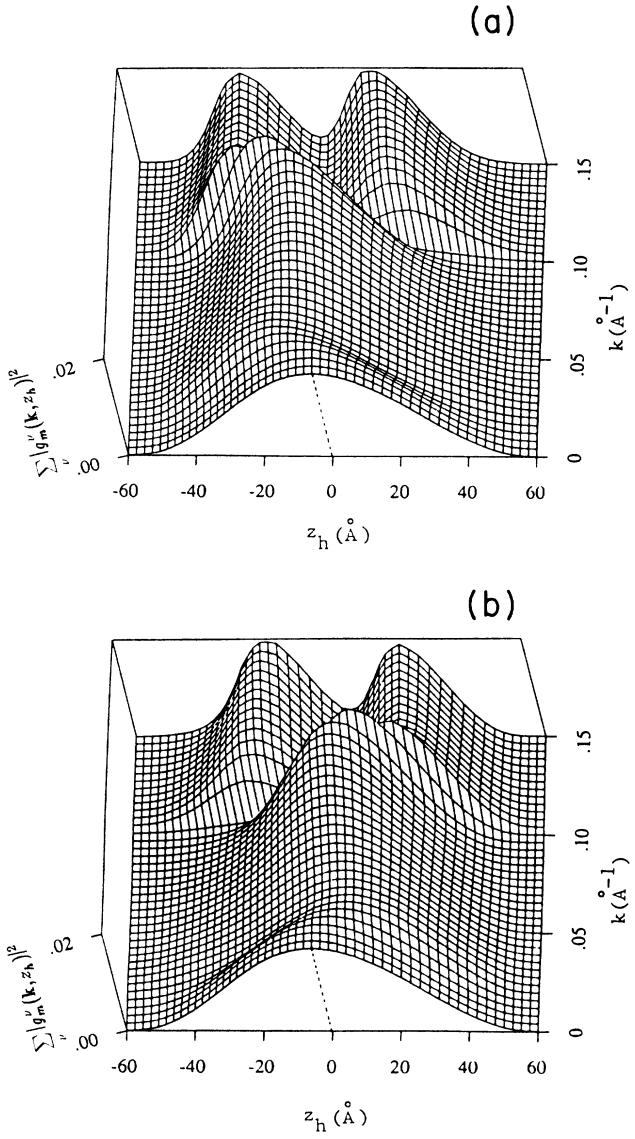

FIG. 2. Hole probability density for the hh1 spin-pair states in a 100-Å $GaAs/Al_{0.3}Ga_{0.7}As$ quantum well.

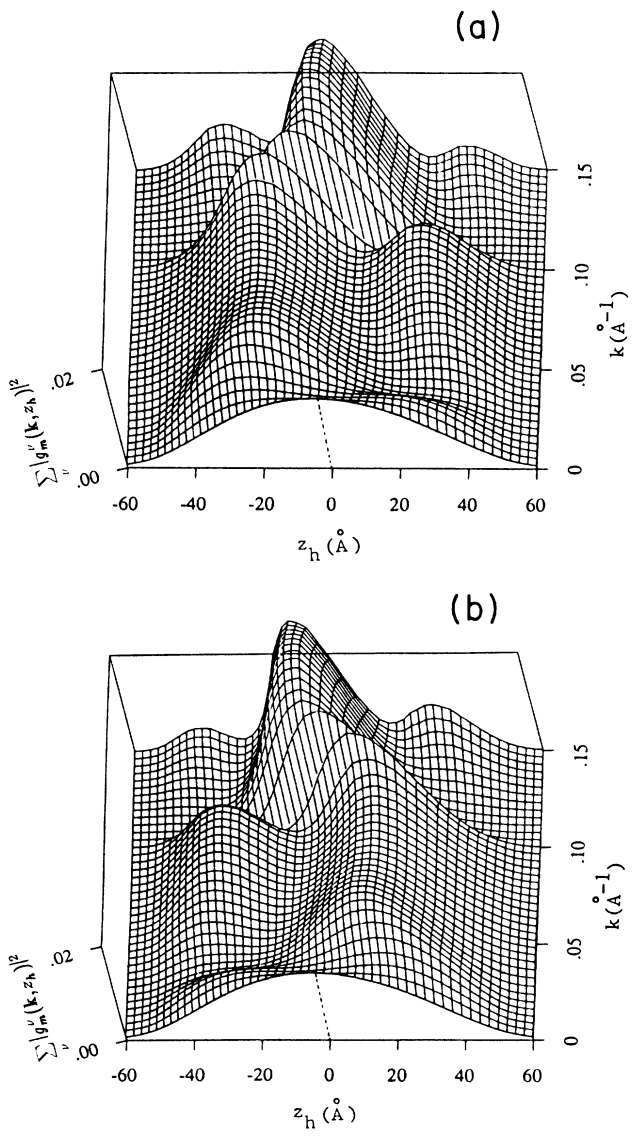

FIG. 3. Hole probability density for the lh1 spin-pair states in a 100-Å $GaAs/Al_{0.3}Ga_{0.7}As$ quantum well.

the full Hamiltonian H becomes

$$H=H^0+V\ , \tag{10}$$

where V is the Coulomb potential described by Eq. (7). To get the acceptor states $|\Psi\rangle$ and energies E we must solve

$$H|\Psi\rangle=E|\Psi\rangle\ . \tag{11}$$

To do this, we expand $|\Psi\rangle$ as

$$|\Psi\rangle=\sum_m \int d\mathbf{k}\,|m,\mathbf{k}\rangle F_m(\mathbf{k})\ . \tag{12}$$

We solve for the expansion coefficients $F_m(\mathbf{k})$ by taking matrix elements of Eq. (11) between states $|m,\mathbf{k}\rangle$ and $|m',\mathbf{k}'\rangle$ using Eq. (7). This results in the eigenvalue equation

$$\sum_{m'} \int d\mathbf{k}' \int dz_h \sum_\nu g_m^{\nu *}(\mathbf{k},z_h)g_{m'}^{\nu}(\mathbf{k}',z_h) \times V(\mathbf{k}-\mathbf{k}';z_i,z_h)F_{m'}(\mathbf{k}')=[E-E_m(\mathbf{k})]F_m(\mathbf{k})\ , \tag{13}$$

where $V(\mathbf{k}-\mathbf{k}';z_i,z_h)$ is given by Eq. (8).

We solve Eq. (13) directly by a finite difference method for singular integral equations; the details of the solution are presented in the Appendix. This approach allows us to maintain the complete generality of the problem and does not require any variational assumptions.

III. THEORETICAL RESULTS

In Fig. 4 we show the calculated acceptor-level energy for the hh1 state as a function of dopant position in a 100-Å GaAs (solid curve) and $In_{0.2}Ga_{0.8}As$ (dotted curve) quantum well bounded by $Al_{0.3}Ga_{0.7}As$. We see that, as expected, the binding energy decreases as the impurity is placed farther from the center of the quantum well. This occurs since the hole probability density function $\sum_\nu |g_m^\nu(\mathbf{k},z_h)|^2$ is maximized at the center of the well; thus, the impurity potential has the greatest effect when the ion is placed there. We also see, however, a splitting of the acceptor levels corresponding to the difference in binding energies between the two different hh1 spin-pair states. This results from the asymmetric z_h dependence

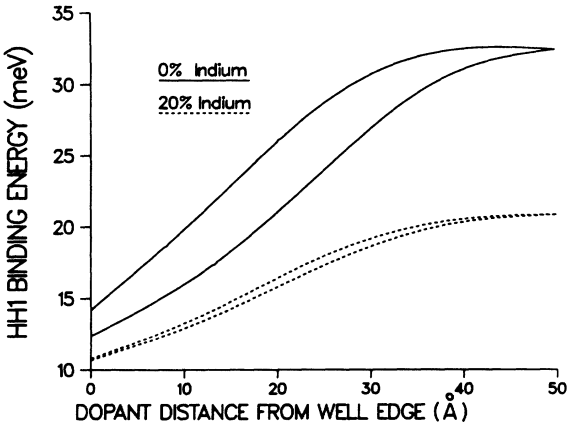

FIG. 4. hh1 acceptor-level binding energy as a function of position of the dopant in a 100-Å GaAs/$Al_{0.3}Ga_{0.7}As$ (solid curve) and $In_{0.2}Ga_{0.8}As/Al_{0.3}Ga_{0.7}As$ (dotted curve) quantum well.

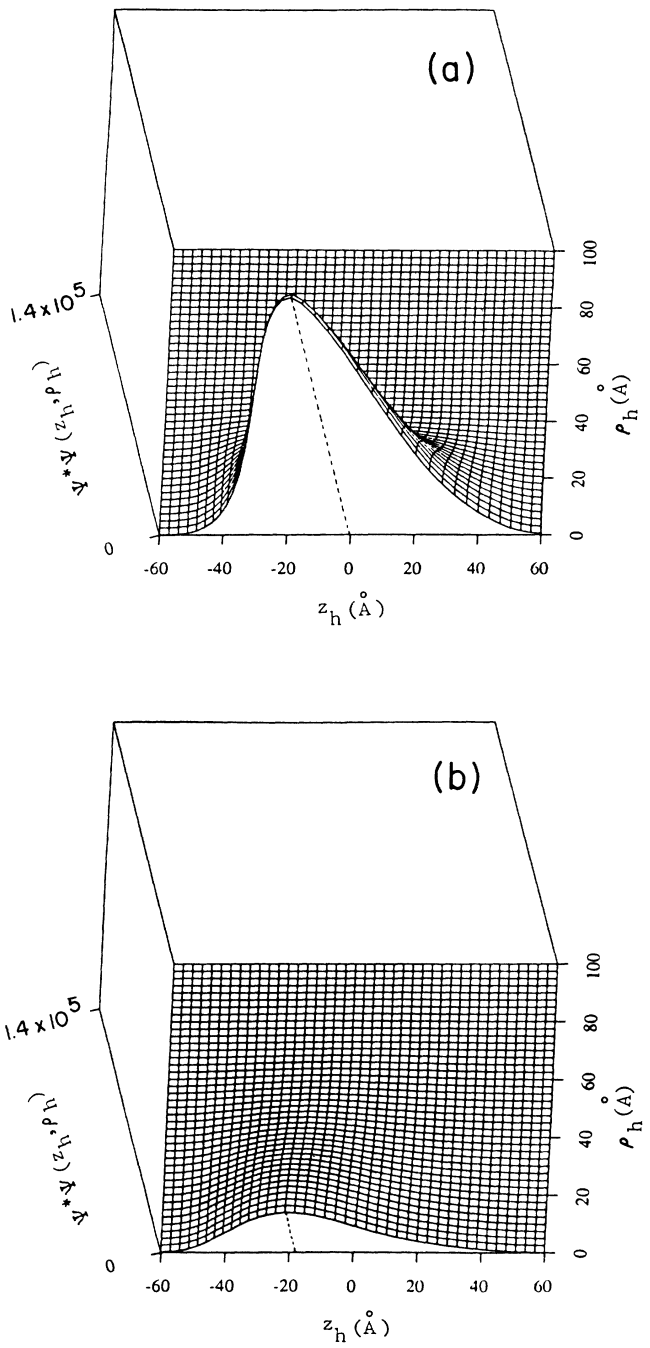

FIG. 5. Probability density function $P(\rho_h,z_h)$ in a 100-Å GaAs/$Al_{0.3}Ga_{0.7}As$ quantum well with the impurity placed at (a) the center of the well ($z=0$) and (b) the edge of the well ($z=-50$ Å).

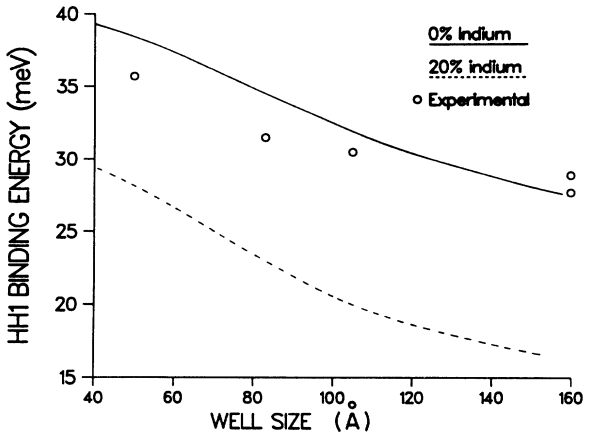

FIG. 6. hh1 acceptor-level binding energy as a function of well width in a $GaAs/Al_{0.3}Ga_{0.7}As$ (solid curve) and $In_{0.2}Ga_{0.8}As/Al_{0.3}Ga_{0.7}As$ (dotted curve) quantum well with the impurity at the center. Experimental points are from Ref. 9.

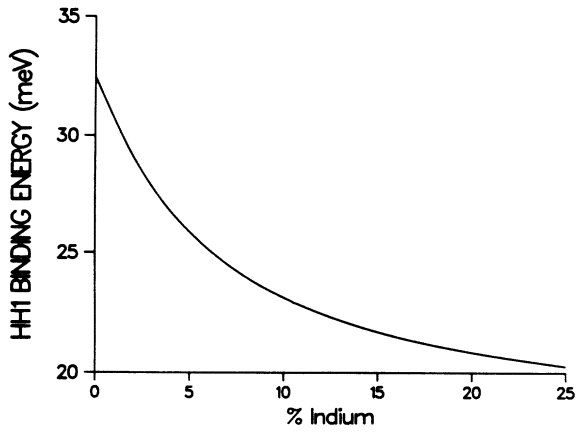

FIG. 7. hh1 acceptor-level binding energy as a function of In content (y) in a 100-Å $In_yGa_{1-y}As/Al_{0.3}Ga_{0.7}As$ quantum well with the impurity at the center.

in the envelope functions shown in Figs. 2 and 3. As the impurity is moved from the center of the quantum well, inversion symmetry is lost and its potential couples more strongly to one of the degenerate states and less strongly to the other, depending on which side of the well the impurity is placed in. Of course, the splitting is reversed if the impurity is moved to the other side of the well. This effect cannot be noticed if we make the zone-center approximation that $\sum_\nu g_m^{\nu *}(\mathbf{k},z_h)g_{m'}^{\nu}(\mathbf{k}',z_h)=\sum_\nu |g_m^{\nu}(0,z_h)|^2$ as other authors[8] have done when solving $\mathbf{k}$-space equations variationally. Hence, we see a *qualitative* difference between variational and numerical solutions.

Figure 5 shows the real-space probability density function for the upper energy hh1 acceptor state for a 100-Å $GaAs/Al_{0.3}Ga_{0.7}As$ quantum well with the impurity placed at (a) the center ($z=0$) and (b) the edge ($z=-50$ Å) of the quantum well. We see that the wave-function shifts to the side of the well and extends farther in ρ_h as the dopant is moved to the edge of the well. This change in the z_h dependence of the acceptor-level wave function comes from the variation with $\mathbf{k}$ of the envelope functions and from the mixing in of higher-order m states. Hence, it is essential to include the coupling between states $m \neq m'$ in Eq. (13) in order to accurately compute the wave function. If the zone-center and uncoupled-subband approximations are made, the z_h dependence will be the same for all dopant positions.

Figure 6 shows the hh1 acceptor-level binding energy for an on-center impurity in a GaAs (solid curve) and $In_{0.2}Ga_{0.8}As$ (dotted curve) quantum well bounded by $Al_{0.3}Ga_{0.7}As$ as a function of well size. Experimental points from Ref. 9 are also plotted for the lattice-matched curve and we see good agreement. Finally, in Fig. 7 we show the effect of strain (In composition) on the hh1 acceptor state in a 100-Å $In_yGa_{1-y}As$ well as a function of y with the dopant in the center. Note that the acceptor-level energy is significantly affected by the strain and can be used as an important signature to characterize the valence-band structure in a strained well.

IV. CONCLUSIONS

In this paper we have addressed the problem of acceptor-level binding energies in pseudomorphically strained $In_yGa_{1-y}As/Al_xGa_{1-x}As$ quantum wells. The acceptor-level energies show a sharp decrease as the strain in the system increases. We note that the decrease is due to the biaxial strain and not due to the addition of In. Although several experimental groups have focused on hole masses in strained quantum wells, the acceptor levels have not been probed. Our studies show that the effect of strain on the acceptor binding energies is quite large and could be used quite effectively to probe the valence-band structure in these strained wells.

ACKNOWLEDGMENTS

The authors thank Dr. M. Jaffe for his help and several useful discussions. This work was funded by the U.S. Army Research Office under Contract No. DAAL03-87-K-0007.

APPENDIX: NONVARIATIONAL NUMERICAL SOLUTION TO THE EIGENVALUE EQUATION

To solve Eq. (13) we first make the assumption that the hole energies and envelope functions depend only on k; thus we expect that the $F_m(\mathbf{k})$ will depend only on the magnitude of $\mathbf{k}$. In addition, we note from Eq. (8) that our potential $V(\mathbf{k}-\mathbf{k}';z_i,z_h)$ depends only on $|\mathbf{k}-\mathbf{k}'|$, so we write $V(|\mathbf{k}-\mathbf{k}'|;z_i,z_h)\equiv V(\mathbf{k}-\mathbf{k}';z_i,z_h)$ and choose our coordinate system so that

$$|\mathbf{k}-\mathbf{k}'|=[k^2+(k')^2-2kk'\cos\theta]^{1/2} . \quad \text{(A1)}$$

With these approximations we can simplify Eq. (13) to

$$\sum_{m'} \int_0^\infty dk' \left[k' \int_0^{2\pi} d\theta \int dz_h \sum_\nu g_m^{\nu *}(k,z_h) g_{m'}^{\nu}(k',z_h) V\{[k^2+(k')^2-2kk'\cos\theta]^{1/2};z_i,z_h\} \right] F_{m'}(k')$$
$$= [E - E_m(k)] F_m(k) . \quad \text{(A2)}$$

We have now reduced the problem to a one-dimensional integral eigenvalue problem, but this is not the most convenient form for numerical treatment. To solve Eq. (A2), we symmetrize the integral kernel by multiplying Eq. (A2) by $\sqrt{k}$ and setting

$$R_m(k) \equiv \sqrt{k} F_m(k) . \quad \text{(A3)}$$

This transformation gives the integral equation

$$\sum_{m'} \int_0^\infty dk' h_{mm'}(k,k') R_{m'}(k') = [E - E_m(k)] R_m(k) , \quad \text{(A4)}$$

where the *Hermitian* kernel is given by

$$h_{mm'}(k,k') \equiv \sqrt{kk'} \int_0^{2\pi} d\theta \int dz_h \sum_\nu g_m^{\nu *}(k,z_h) g_{m'}^{\nu}(k',z_h) V\{[k^2+(k')^2-2kk'\cos\theta]^{1/2};z_i,z_h\} . \quad \text{(A5)}$$

We solve Eq. (A4) by breaking up the k axis up into discrete intervals of width Δk and by assuming that $h_{mm'}(k,k')$ and $R_m(k)$ are constant over each interval. This discretization yields a Hermitian matrix which we diagonalize to get the eigenvalue E and the eigenvector $R_m(k)$. We see from Eq. (8), however, that the bare Coulomb potential $V(\mathbf{k}-\mathbf{k}';z_i,z_h)$ is singular at $\mathbf{k}=\mathbf{k}'$. Since the $|\mathbf{k}-\mathbf{k}'|^{-1}$ singularity occurs in two dimensions, though, it is integrable and Eq. (A4) has well-defined solutions. To find these solutions by a discretization of Eq. (A4), we must treat the interval where $k=k'$ carefully. Instead of approximating $h_{mm'}(k,k')$ on this interval by its $k=k'$ value, we must integrate the singularity and use the *average* value

$$\bar{h}_{mm'}(k,k) \equiv \frac{1}{\Delta k} \int_{k-(\Delta k/2)}^{k+(\Delta k/2)} dk' h_{mm'}(k,k')$$
$$\approx \frac{-e^2}{2\pi\epsilon} \int dz_h \sum_\nu g_m^{\nu *}(k,z_h) g_{m'}^{\nu}(k,z_h) \frac{1}{\Delta k} \int_{k-(\Delta k/2)}^{k+(\Delta k/2)} dk' \sqrt{kk'} \int_0^{2\pi} d\theta \frac{e^{[k^2+(k')^2-2kk'\cos\theta]^{1/2}|z_i-z_h|}}{[k^2+(k')^2-2kk'\cos\theta]^{1/2}} . \quad \text{(A6)}$$

We are interested in the two inner integrals

$$I(k;z_i,z_h) \equiv \frac{1}{\Delta k} \int_{k-(\Delta k/2)}^{k+(\Delta k/2)} dk' \sqrt{kk'} \int_0^{2\pi} d\theta \frac{e^{[k^2+(k')^2-2kk'\cos\theta]^{1/2}|z_i-z_h|}}{[k^2+(k')^2-2kk'\cos\theta]^{1/2}} . \quad \text{(A7)}$$

Note that the region of integration used to define I is an annulus in the $\mathbf{k}$ plane of thickness Δk and radius k. Since the integrand in Eq. (A7) is only singular when $k=k'$ *and* $\theta=0$, we choose a small enough $\Delta\theta$ such that the singularity is confined to the region where $-\Delta\theta \le \theta \le \Delta\theta$; the precise meaning of this will be made clear later. We then write I as

$$I(k;z_i,z_h) = \frac{1}{\Delta k} \int_{k-(\Delta k/2)}^{k+(\Delta k/2)} dk' \sqrt{kk'} \int_{\Delta\theta}^{2\pi-\Delta\theta} d\theta \frac{e^{[k^2+(k')^2-2kk'\cos\theta]^{1/2}|z_i-z_h|}}{[k^2+(k')^2-2kk'\cos\theta]^{1/2}}$$
$$+ \frac{1}{\Delta k} \int_{k-(\Delta k/2)}^{k+(\Delta k/2)} dk' \sqrt{kk'} \int_{-\Delta\theta}^{\Delta\theta} d\theta \frac{e^{[k^2+(k')^2-2kk'\cos\theta]^{1/2}|z_i-z_h|}}{[k^2+(k')^2-2kk'\cos\theta]^{1/2}} . \quad \text{(A8)}$$

Since $\Delta\theta$ is small and the region of integration on the k axis is small, we assume $k \approx k'$ everywhere in the first term of Eq. (A8) to get

$$\sqrt{kk} \int_{\Delta\theta}^{2\pi-\Delta\theta} d\theta \frac{e^{(k^2+k^2-2kk\cos\theta)^{1/2}|z_e-z_h|}}{(k^2+k^2-2kk\cos\theta)^{1/2}} . \quad \text{(A9)}$$

Now the singularity is confined to the region of integration in the second term of Eq. (A8) which we denote by D; note that D is shaped like a polar volume element. Since $\Delta\theta$ is small, the area A of this region D is approximately the area of a polar volume element ($dA = r\,dr\,d\theta$) so that we have ($r \to k$, $dr \to \Delta k$, $d\theta \to 2\,\Delta\theta$)

$$A \approx 2k\,\Delta k\,\Delta\theta . \quad \text{(A10)}$$

Now since $\Delta\theta$ was chosen very small, our region D looks almost like a rectangle with height $2k\,\Delta\theta$ and width Δk; we choose this rectangle to be a square so we set

$$2k\,\Delta\theta = \Delta k \Longrightarrow \Delta\theta = \frac{\Delta k}{2k} . \quad \text{(A11)}$$

Thus, given a small step size Δk and a particular value of k, a small $\Delta\theta$ is determined. We are still faced with the problem of evaluating the second term of Eq. (A8),

$$\frac{1}{\Delta k}\int_{k-(\Delta k/2)}^{k+(\Delta k/2)} dk'\sqrt{kk'}\int_{-\Delta\theta}^{\Delta\theta} d\theta \frac{e^{[k^2+(k')^2-2kk'\cos\theta]^{1/2}|z_i-z_h|}}{[k^2+(k')^2-2kk'\cos\theta]^{1/2}} . \tag{A12}$$

To do this, we first approximate $k\approx k'$ everywhere but in the denominator and assume that the exponential factor changes little from its $k=k',\theta=0$ value of 1. This gives

$$\text{2nd term}\approx\frac{1}{\Delta k}\int_{k-(\Delta k/2)}^{k+(\Delta k/2)} dk'\sqrt{k'k'}\int_{-\Delta\theta}^{\Delta\theta} d\theta \frac{1}{[k^2+(k')^2-2kk'\cos\theta]^{1/2}}$$
$$=\frac{1}{\Delta k}\int_D d\mathbf{k}'\frac{1}{|\mathbf{k}-\mathbf{k}'|} . \tag{A13}$$

To evaluate the integral in Eq. (A13) we approximate the region D by a disk D' of radius η centered at the point where $\mathbf{k}=\mathbf{k}'$ and having the same area as D. Thus we choose η so that

$$\pi\eta^2=2k\,\Delta k\,\Delta\theta\Longrightarrow\eta=\frac{\Delta k}{\sqrt{\pi}} , \tag{A14}$$

where Eq. (A11) was used. We now approximate

$$\frac{1}{\Delta k}\int_D d\mathbf{k}'\frac{1}{|\mathbf{k}-\mathbf{k}'|}\approx\frac{1}{\Delta k}\int_{D'} d\mathbf{k}'\frac{1}{|\mathbf{k}-\mathbf{k}'|} . \tag{A15}$$

We have made this approximation as good as possible by choosing the region D to be squarelike, thereby making its shape as much like a circle as any polar volume element shaped region can be. Finally, we shift to local coordinates by setting $\mathbf{u}\equiv\mathbf{k}-\mathbf{k}'$. We can then evaluate the integral over D' as

$$\frac{1}{\Delta k}\int_{D'} d\mathbf{u}\frac{1}{|\mathbf{u}|}=\frac{1}{\Delta k}\int_0^{\eta} du\,u\int_0^{2\pi} d\theta_u\frac{1}{u}=\frac{2\pi\eta}{\Delta k}=2\sqrt{\pi} . \tag{A16}$$

Thus we have now evaluated

$$I(k;z_i,z_h)=\sqrt{kk}\int_{\Delta k/2k}^{2\pi-(\Delta k/2k)}\frac{e^{[k^2+k^2-2kk\cos\theta]^{1/2}|z_i-z_h|}}{[k^2+k^2-2kk\cos\theta]^{1/2}}d\theta+2\sqrt{\pi} \tag{A17}$$

which we can use to evaluate

$$\bar{h}_{mm'}(k,k)=\frac{-e^2}{2\pi\epsilon}\int dz_h\sum_{\nu} g_m^{\nu*}(k,z_h)g_{m'}^{\nu}(k,z_h)I(k;z_i,z_h) . \tag{A18}$$

This method gives excellent agreement with analytic solutions when it is applied to two- and three-dimensional hydrogen atoms. Therefore, since the two-dimensional hydrogen atom has the same $|\mathbf{k}-\mathbf{k}'|^{-1}$ singularity as Eq. (7), we expect the method to give accurate solutions to the acceptor problem.

After we solve Eq. (A4) for $R_m(k)$, we can use Eqs. (12) and (A3) to get the real-space probability density function $P(\mathbf{r}_h)$. It is given by

$$P(\mathbf{r}_h)\equiv\langle\Psi|\delta(\mathbf{r}-\mathbf{r}_h)|\Psi\rangle=\sum_m\int d\mathbf{k}\,F_m^*(\mathbf{k})\sum_{m'}\int d\mathbf{k}'F_{m'}(\mathbf{k}')\langle m,\mathbf{k}|\delta(\mathbf{r}-\mathbf{r}_h)|m',\mathbf{k}'\rangle$$
$$=\int dk\,\sqrt{k}J_0(k\rho_h)\int dk'\sqrt{k'}J_0(k'\rho_h)\sum_m R_m^*(k)\sum_{m'}R_{m'}(k')\sum_{\nu}g_m^{\nu*}(k,z_h)g_{m'}^{\nu}(k',z_h) . \tag{A19}$$

where J_0 is the zeroth-order Bessel function and the angular integrals were evaluated with the aid of Ref. 10.

[1] J. Matthews and A. Blakeslee, J. Cryst. Growth **27**, 118 (1974).
[2] G. Osbourn, J. Schirber, T. Drummond, L. Dawson, B. Doyle, and I. Fritz, Appl. Phys. Lett. **49**, 731 (1986).
[3] H. Kato, N. Iguchi, S. Chika, M. Nakayama, and N. Sano, J. Appl. Phys. **59**, 588 (1986).
[4] M. Jaffe and J. Singh, J. Appl. Phys. **65**, 329 (1989).
[5] M. Jaffe, J. E. Oh, J. Pamulapati, J. Singh, and P. Bhattacharya, Appl. Phys. Lett. **54**, 2345 (1989).
[6] W. T. Masselink, Y. C. Chang, and H. Morkoç, Phys. Rev. B **28**, 7373 (1983).
[7] J. M. Luttinger and W. Kohn, Phys. Rev. **97**, 869 (1955).
[8] G. D. Sanders and Y. C. Chang, Phys. Rev. B **35**, 1300 (1987).
[9] R. C. Miller, A. C. Gossard, W. T. Tsang, and O. Munteanu, Phys. Rev. B **25**, 3871 (1982).
[10] I. S. Gradshteyn and I. M. Ryzhik, *Table of Integrals, Series, and Products* (Academic, London, 1980), p. 309.